MASTER COPY KEEP THIS COPY FOR REPRODUCTION PURPOSES

REPORT DOCUMENTATION PAGE

Form Approved
OMB No. 0704-0188

1. AGENCY USE ONLY (Leave blank)	2. REPORT DATE	3. REPORT TYPE AND DATES COVERED
	18 November 1994	Technical

4. TITLE AND SUBTITLE

Extension of the "Pore tree" Model to Describe Convection

5. FUNDING NUMBERS

DAAH04-94-C-0075

6. AUTHOR(S)

Girard A. Simons

7. PERFORMING ORGANIZATION NAME(S) AND ADDRESS(ES)

Simons Research Associates
3 Juniper Road
Lynnfield, MA 01940-2416

8. PERFORMING ORGANIZATION REPORT NUMBER

9. SPONSORING / MONITORING AGENCY NAME(S) AND ADDRESS(ES)

U.S. Army Research Office
P.O. Box 12211
Research Triangle Park, NC 27709-2211

10. SPONSORING / MONITORING AGENCY REPORT NUMBER

ARO 32900.3-GS-S

11. SUPPLEMENTARY NOTES

The views, opinions and/or findings contained in this report are those of the author(s) and should not be construed as an official Department of the Army position, policy, or decision, unless so designated by other documentation.

12a. DISTRIBUTION / AVAILABILITY STATEMENT

Approved for public release; distribution unlimited.

12b. DISTRIBUTION CODE

13. ABSTRACT *(Maximum 200 words)*

The "pore tree" model of pore structure (Simons and Finson, 1979; Simons, 1982) was developed for catalysts and sorbents to allow diffusion within a porous media in the absence of convection through the media. The pore tree model is extended herein to describe the permeable pore structure which characterizes the subsurface flow of water in soil, the dispersion of contaminants and the in-situ remediation of contaminated sites. Permeability requires a statistical determination of the "branches" that are common to several trees to allow percolation through the large scale (mobile) structure in addition to diffusion through the smaller scale (immobile) structure. While permeability is dominated by the largest pores, it is important to determine the level of convection that is occurring at the intermediate scales in order to accurately describe transport.

This and subsequent interim technical reports will be self contained in that each report will contain the previous report plus new work described in the last 3-4 pages of each report.

14. SUBJECT TERMS	15. NUMBER OF PAGES
Pore Structure, Interconnectivity, Permeability, Pore Tree	15
	16. PRICE CODE

17. SECURITY CLASSIFICATION OF REPORT	18. SECURITY CLASSIFICATION OF THIS PAGE	19. SECURITY CLASSIFICATION OF ABSTRACT	20. LIMITATION OF ABSTRACT
UNCLASSIFIED	UNCLASSIFIED	UNCLASSIFIED	UL

EXTENSION OF THE "PORE TREE" MODEL TO DESCRIBE CONVECTION

Technical Report

Girard A. Simons

18 November 1994

U.S. Army Research Office

Contract/Grant Number DAAH04-94-C-0075

Simons Research Associates
3 Juniper Road
Lynnfield, MA 01940-2416

THE VIEWS, OPINIONS, AND/OR FINDINGS CONTAINED IN THIS REPORT ARE THOSE OF THE AUTHOR AND SHOULD NOT BE CONSTRUED AS AN OFFICIAL DEPARTMENT OF THE ARMY POSITION, POLICY, OR DECISION, UNLESS SO DESIGNATED BY OTHER DOCUMENTATION.

TABLE OF CONTENTS

TABLE OF CONTENTS 1

I. INTRODUCTION 2

II. ISOLATED PORE TREE: THE STRUCTURE 3

III. INTERCONNECTIVITY 7

IV. CONVECTION IN THE PORE TREE 10

V. SUMMARY 14

VI. REFERENCES 14

I. INTRODUCTION

To properly describe chemical reactions in non-permeable porous media, the "pore tree" was introduced by Simons and Finson (1979) and Simons (1982). This pore structure was developed via analogy to the kinetic theory of gases: the pore length is analogous to the mean free path and under the assumption that the pore aspect ratio (pore length to radius) is a constant, a pore size distribution was obtained that has been confirmed for coal, coal char, sorbents, catalysts and even for kidney stones from both men (low porosity oxalate) and women (high porosity phosphate). The pore tree was statistically derived from the pore size distribution and allows the orderly migration of a reactant gas from the large pores to the small pores (see Fig. 1). A detailed description of the pore tree and the coupled transport and chemistry is given by Simons (1982, 1983a). The spatially dependent transport/reaction equations are solved for a single pore tree and then the total contribution of all trees (of all sizes) in the system is obtained by summing the contribution of each tree that reaches the exterior of the system. This is distinct from the "bulk" transport equations that integrate over all pores at a fixed point in space before they integrate spatially. The "bulk" transport approach inherently assumes instantaneous mixing between large and small pores at a single point in space (Random Pore Models) while the pore tree relaxes this assumption with a structure that is developed statistically and is relatively easy to work with mathematically.

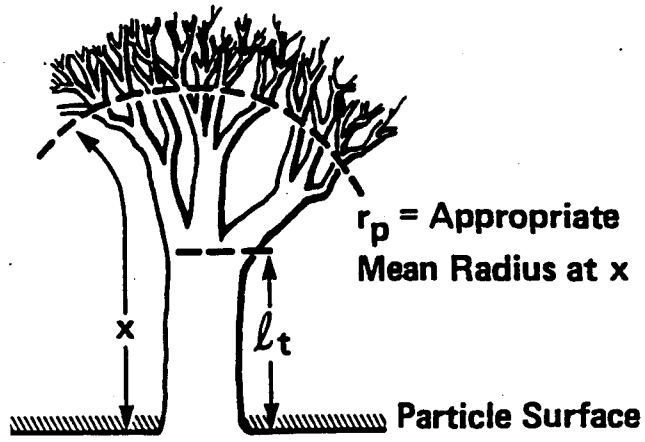

Figure 1. The Pore Tree

In all previous applications (sorbents, catalysts and coal combustion) the pore tree represents an isolated sub-structure, allowing diffusion into and out of the porous media without permitting convection through the media. Under the current ARO program, Simons Research Associates is adapting its pore tree model to describe the permeable pore structure and convective transport characteristic of the subsurface flow of water in soil, the dispersion of contaminants and the in-situ remediation of contaminated sites. The random nature of the pore structure, which formed the basis of the statistical derivation of the pore tree, is applied to the underground structure of porous soil, sand and rocks. The statistical description of the pore tree is extended to describe the concept of permeability, thus allowing convective flow as a transport mechanism in addition to the diffusive transport already considered. Physically, this amounts to statistically determining the "branches" that are common to several trees to allow percolation through the large scale (mobile) structure in addition to diffusion through the smaller scale (immobile) structure. While permeability is dominated by the largest pores, it is important to determine the level of convection that is occurring at the intermediate scales in order to accurately describe transport. The resulting pore structure will provide an analytic description of an underground network upon which transport and coupled chemical reactions may be accurately superimposed.

II. ISOLATED PORE TREE: THE STRUCTURE

Following the pore structure theory of Simons and Finson (1979) and Simons (1982), consider a spherical porous particle of radius a, containing pores of length l_p and radius r_p. The pore dimensions range from a microscale of the order of Ångstroms to a macroscale which is a significant fraction of the particle radius. The radius of the largest pore is denoted by r_{max} and is given by

$$r_{max}=2a\theta^{1/3}/3K_o \tag{1}$$

where θ is the total porosity of the particle and K_o is a constant of integration, approximately equal to five, which relates the pore length to its radius

$$l_p=K_o r_p/\theta^{1/3} \tag{2}$$

The radius of the smallest pore is denoted by r_{min} and is given by

$$r_{min}=2\theta/\beta\rho_s s_p \tag{3}$$

where ρ_s is the density of the solid matrix, s_p is the specific internal surface area (several hundred m^2/g), and

$$\beta=\ln(r_{max}/r_{min}) \tag{4}$$

The particle contains a continuous distribution of pore sizes from r_{min} to r_{max} . The number of pores within an arbitrary plane of cross-sectional area A and with radius between r_p and $r_p + dr_p$ is denoted by $\bar{g}(r_p)Adr_p$. The pore distribution function $\bar{g}(r_p)$ is given by

$$\bar{g}(r_p)=\theta/2\pi\beta r_p^3 \tag{5}$$

where $\bar{g}(r_p)$ indicates an average over all inclination angles between the axis of the pore and the normal to the plane. Due to the random orientation of the pores, the intersection of a circular cylinder with a plane is an ellipse of average area $2\pi r_p^2$. Hence, the porosity is the $2\pi r_p^2$ moment of $\bar{g}(r_p)$ and the internal surface area is the $4\pi r_p$ moment of $\bar{g}(r_p)$. The expression for $\bar{g}(r_p)$ was derived (Simons and Finson,1979) from statistical arguments and has been validated through extensive comparison of the predicted volume and surface area distributions with mercury intrusion data (Stacy and Walker, 1972). This has been accomplished for coal, char derived from that coal (Kothandaraman et.al., 1984), sorbents, catalysts and even kidney stones from both men (oxalate) and women (phosphate).

A characteristic feature of the $1/r_p^3$ distribution depicts that the pore volume between r_{min} and r_p increases linearly with the natural log of r_p. It is the functional form of this relationship,

$$Pore\ Volume \propto \int_{r_{min}}^{r_p} r_p^2 \bar{g}(r_p) dr_p \propto \ln r_p \tag{6}$$

that depicts the inverse cubic dependence of $\bar{g}(r_p)$ on r_p. A linear display of mercury intrusion volume vs. $\ln(r_p)$ always infers a $1/r_p^3$ distribution.

The number of pores within the bulk volume V whose pore radius is between r_p and $r_p + dr_p$ may be defined by $Vf(r_p)dr_p$. The pore volume is expressed as the $\pi r_p^2 l_p$ moment of $f(r_p)$ and the internal surface area is the $2\pi r_p l_p$ moment of $f(r_p)$. The pore size distribution functions ($f(r_p)$ and $\bar{g}(r_p)$) are clearly not independent. The definitions of porosity and internal surface area infer that $f(r_p)$ is related to $\bar{g}(r_p)$ by

$$\bar{g}(r_p) = f(r_p) l_p / 2 \tag{7}$$

Equation (7) simply states that the probable number of pores intersecting an arbitrary plane increases with the length of the pore and with the density of pores.

The length of a pore is determined by an arbitrary intersection with another pore and is expressed (Simons and Finson, 1979) as a collision integral over the pore distribution functions. The analysis suggests that l_p , $\bar{g}(r_p)$ and $f(r_p)$ are proportional to r_p , $1/r_p^3$ and $1/r_p^4$ respectively. The constants of proportionality are obtained from integral constraints, i.e., the total porosity and internal surface area contained in the pore structure. The expression for $f(r_p)$ is given by

$$f(r_p) = \frac{\theta^{4/3}}{\pi \beta K_o r_p^4} \tag{8}$$

where the constants were defined above.

The pore volume distribution corresponding to these distribution functions is similar to that utilized in the random pore model (Gavalas, 1980 & 1981). However, the pore tree model and the random pore model differ dramatically in their choice of the pore aspect ratio (length to diameter) and its implications with respect to pore branching. The random pore model allows a single pore to connect two larger pores. This picture lends itself to the idealization of instantaneous mixing between the pores and requires that the pore aspect ratio be of the order of one hundred. The pore tree theory uses data for r_{max} to imply (via K_o) that

all pores possess an aspect ratio of the order of ten. Hence, small pores may connect to larger pores only on one end and all pores must branch from successively larger pores like a tree or river system.

Each pore that reaches the exterior surface of the particle is depicted as the trunk of a tree. The size distribution of tree trunks on the exterior surface of the particle is denoted by $\bar{g}(r_t)4\pi a^2 dr_t$ where $\bar{g}(r_t)$ is functionally identical to $\bar{g}(r_p)$. Each trunk of radius r_t is associated with a specific tree-like structure. Let N_t be defined as the branch distribution function where $N_t dr_p$ is the number of pores of radius r_p (within size range dr_p) in a tree whose trunk radius is r_t. The total number of pores of radius r_p in a sphere of radius a may be expressed as $4/3\pi a^3 f(r_p)dr_p$ or, as the sum of all pores of radius r_p contained within every tree in the porous sample, plus all pores of radius r_p that are themselves the trunk of a tree. Hence,

$$\frac{4}{3}\pi a^3 f(r_p) = \int_{r_p}^{r_{max}} N_t \bar{g}(r_t) 4\pi a^2 dr_t + 4\pi a^2 \bar{g}(r_p) \tag{9}$$

where $\bar{g}(r_t)$ is the number of tree trunks per unit external area of the porous sample and only those trees whose trunk radius is greater than r_p may contain a pore of radius r_p. Using the previously derived expressions for r_{max}, $\bar{g}(r_p)$ and $f(r_p)$, Eq.(9) is identically satisfied by

$$N_t = r_t^3 / r_p^4 \tag{10}$$

The branch distribution function completely characterizes the pore tree. The internal surface area and pore volume associated with each pore tree are denoted by $S_t(r_t)$ and $V_t(r_t)$, respectively, and are expressed as the sum of the contributions from the trunk and that from the branches.

$$S_t(r_t) = 2\pi r_t l_t + \int_{r_{min}}^{r_t} 2\pi r_p l_p N_t dr_p \tag{11}$$

$$V_t(r_t) = \pi r_t^2 l_t + \int_{r_{min}}^{r_t} \pi r_p^2 l_p N_t dr_p \tag{12}$$

Using Eq.(10) for N_t, $S_t(r_t)$ and $V_t(r_t)$ become

$$S_t(r_t)=2\pi r_t l_t\left(\frac{r_t}{r_{min}}\right)(1-\theta) \tag{13}$$

$$V_t(r_t)=\pi r_t^2 l_t\left(1+\ln\left(\frac{r_t}{r_{min}}\right)\right) \tag{14}$$

where the $(1-\theta)$ term in S_t has been included to account for pore combination (Simons, 1979a).

The surface area associated with the pore tree may be several orders of magnitude greater than the surface area of the trunk. However, the volume of the pore tree may, at most, be one order of magnitude greater than that of the trunk. It should also be noted that the above expressions for S_t and V_t reduce to those appropriate to a single cylindrical pore in the limit of $r_t \rightarrow r_{min}$ (the leaf of the tree). Furthermore, the integrals of $S_t(r_t)$ and $V_t(r_t)$ over all $\bar{g}(r_t)$ recover the total internal surface area and pore volume of the porous sample.

Each trunk of radius r_t is associated with a specific tree-like structure with continuous branching to ever decreasing pore radii. The radius and number of pores is a unique function of the distance x into the tree. The coordinate x is skewed in that it follows a tortuous path through the branches of the tree. Let n(x) represent the number of pores of radius r_p at location x in a tree of trunk radius r_t. An analysis (Simons,1982) of this pore tree has demonstrated that

$$n(x)=r_t^2/r_p^2(x) \tag{15}$$

and the coordinate x is related to r_p by

$$dr_p/dx=-r_p/l_t \tag{16}$$

The continuous branching model has been used to successfully describe char oxidation (Lewis and Simons, 1979; Simons, 1982 & 1983a), coal pyrolysis (Simons, 1983b & 1984) and the catalytic cracking of benzene by porous iron oxides (Simons et al., 1986). It was also used to successfully describe sulfur sorption (SO_2 and H_2S) by porous calcine (CaO) in the limit of zero utilization (Simons and Rawlins, 1980; Simons et al., 1984) and was later extended to include $CaSO_4$ and CaS deposits (Simons and Garman, 1986; Simons et al., 1987; Simons, 1988; Simons et al., 1988). The subsequent determination of the controlling physical parameters led to a new concept for the optimization of the sulfur sorption process (Simons, 1991; Simons et al., 1992) through spray drying of water soluble organic calcium solutions to control the sorbent pore structure.

III. INTERCONNECTIVITY

The first step in determining the size distribution of the interconnected pores and the distribution of the permeability is to determine the distribution function $\bar{G}_t(r_t,r_p)dr_p$ which represents the number of pores of radius r_p (within size range dr_p) per unit cross section of an arbitrary plane and also contained within a tree whose trunk radius is r_t. Consider an infinite homogeneous isotropic porous media and isolate a spherical volume of that media denoted by the radius a. Such a volume is illustrated in Fig. 2. The total number of pores of radius r_p (within size range dr_p) intersecting plane AA of area πa^2 has previously been defined by $\bar{g}(r_p)\pi a^2 dr_p$. The pores in plane AA in this size range may also be determined by integrating $\bar{G}_t(r_t,r_p)\pi a^2 dr_p$ over all trees whose trunk intersects the exterior surface of the porous sample. Hence it follows that

$$\bar{g}(r_p)\pi a^2 dr_p = \int_{r_p}^{r_{max}} [\bar{G}_t(r_t,r_p)\pi a^2 dr_p]\,\bar{g}(r_t)4\pi a^2 dr_t \tag{17}$$

where only those trees whose trunk radius is greater than r_p may contain a pore of radius r_p.

A solution to Eq. (17) for $\bar{G}_t(r_t,r_p)$ will not necessarily be unique. Physical arguments will help determine $\bar{G}_t(r_t,r_p)$ and help ensure that it is the particular solution we seek. Since N_t represents the number of pores of size r_p in the tree and the probability of a pore intersecting a plane is proportional to its length, it follows that $\bar{G}_t(r_t,r_p)$ should be

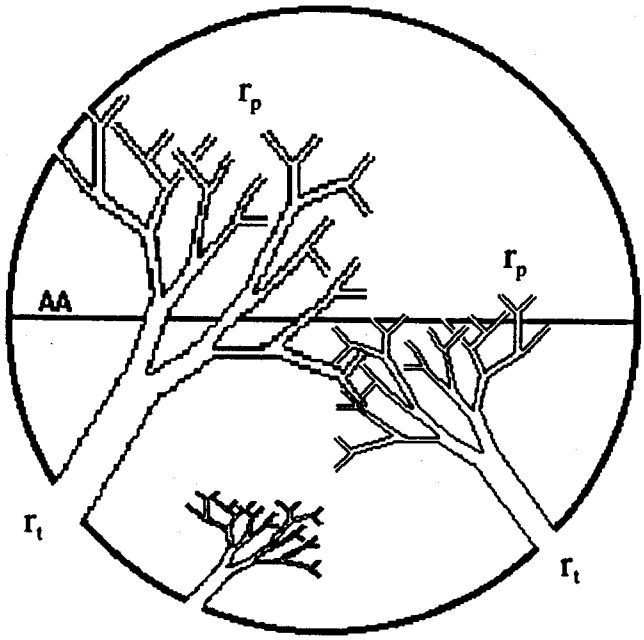

Figure 2. Spherical Volume of a Porous Media

proportional to the product of N_t and l_p/l_t , i.e., proportional to r_t^2/r_p^3. Eq. (17) is identically satisfied by a function which differs from r_t^2/r_p^3 by $\ln(r_p)$.

$$\bar{G}_t(r_t, r_p) = \frac{r_t^2}{4\pi a^2 r_p^3 \ln(r_{max}/r_p)} \tag{18}$$

Note that $\ln(r_p/r_{max})$ introduces an integrable singularity at $r_p = r_{max}$ such that $\bar{G}_t(r_t, r_p)\, dr_p$ is finite at $r_p = r_{max}$. Hence, there is one and only one largest pore for each reference sphere.

Further confirmation of the form for $\bar{G}_t(r_t, r_p)$ may be made through the definitions of porosity and internal surface area. If the porosity and internal surface area in plane AA due to a single tree of radius r_t are defined by

$$\theta_t = \int_{r_{min}}^{r_t} \bar{G}_t(r_t, r_p) 2\pi r_p^2 dr_p \approx \frac{r_t^2}{2a^2} \tag{19}$$

and

$$s_t = \int_{r_{min}}^{r_t} \frac{1}{\rho_s} \bar{G}_t(r_t, r_p) 4\pi r_p dr_p \approx \frac{r_t^2}{\rho_s a^2 \beta r_{min}} \tag{20}$$

respectively, then the total porosity and internal surface area must be represented by their respective integrals of θ_t and s_t over all trees. Hence θ

$$\theta = \int_{r_{min}}^{r_{max}} \theta_t \bar{g}(r_t) 4\pi a^2 dr_t \tag{21}$$

and s_p

$$s_p = \int_{r_{min}}^{r_{max}} s_t \bar{g}(r_t) 4\pi a^2 dr_t \tag{22}$$

follow respectively.

It is stated without further proof that Eqs. (19) to (22) are compatible in both their exact and their approximate forms. The distribution function $\bar{G}_t(r_t, r_p)$ as given by Eq. (18)

is exact and will be used to determine the interconnectivity of the pore structure.

The probability of trees sharing common branches, i.e., the interconnectivity of the pore structure is described in Fig. 3. We seek the distribution function $\bar{I}(r_p)dr_p$ which represents the number of pores (within size range dr_p about r_p) per unit area of plane AA that are connected to both sides of the pore structure through pores at least as large as r_p. A_θ is defined as the area within plane AA that is **open to one side** of the porous media through all trees of size r_t' (through all pores of size r_p' that are at least as large as r_p). Subsequently, $A_\theta \bar{G}_t(r_t, r_p)dr_p$ represents the number of pores of size r_p (within size range dr_p) per unit area of plane AA that are contained in a tree of size range dr_t about r_t **and are also connected to the opposite side of the porous media** through all trees denoted by r_t'. It follows that the distribution function for interconnected pores in plane AA may be obtained by integrating $A_\theta \bar{G}_t(r_t, r_p)dr_p$ over all trees (r_t) that are large enough to contain a pore of size r_p . Hence,

$$\bar{I}(r_p)\pi a^2 dr_p = \int_{r_p}^{r_{max}} [A_\theta \bar{G}_t(r_t, r_p)dr_p]\, \bar{g}(r_t)\, 2\pi a^2 dr_t \tag{23}$$

From the above definition of A_θ , A_θ may be expressed as

$$A_\theta = \int_{r_p}^{r_{max}} [\int_{r_p}^{r_t} 2\pi r_p^2\, \pi a^2 \bar{G}_t(r_t, r_p)\, dr_p]\, \bar{g}(r_t) 2\pi a^2 dr_t \tag{24}$$

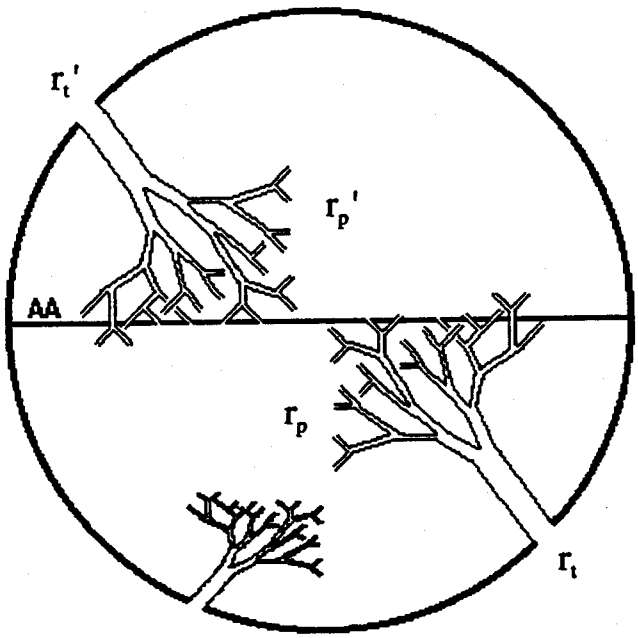

Figure 3. Interconnectivity of a Porous Media

where the primes on the variables of integration have been omitted. Evaluating Eq. (24) yields

$$A_\theta = \frac{\pi a^2 \theta \ln(r_{max}/r_p)}{2\beta} \tag{25}$$

from which Eq. (23) yields the common branch distribution function.

$$\bar{I}(r_p) = \frac{\theta \ln(r_{max}/r_p)}{4\beta} \bar{g}(r_p) \tag{26}$$

It has been deduced that the total number of common branches of size r_p in an arbitrary plane scales approximately with the total number of pores of that size in that plane. Hence, there is a probability of interconnectivity at pore size r_p that is logarithmic in pore size. Defining this probability as $P_I(r_p)$ via Eq. (26),

$$P_I(r_p) = \frac{\theta \ln(r_{max}/r_p)}{4\beta} \tag{27}$$

it is apparent that approximately one percent of all pores of all sizes are interconnected through larger pores. Hence, convection will be responsible for transport in approximately one percent of the small pores. While permeability is dominated by the largest pores, it is important to determine the level of convection that is occurring in smaller pores in order to accurately describe the fine scale transport necessary to assess chemical reactions. The broad size range associated with the interconnectivity suggests that a very wide range of pore sizes separates the "mobile" and "immobile" regions of the pore structure and that a complicated mixture of convective and diffusive transport persists in this pore size range. Determining permeability as a function of pore size is the first step in describing the transport in this pore size range.

IV. CONVECTION IN THE PORE TREE

Convection across plane AA in Fig. 4 will possess contributions from three sources illustrated in Figs. 4a, 4b and 4c. Fig. 4a illustrates the case where the convection in plane AA is due solely to the pores that are interconnected in that plane. Fig. 4b illustrates the case where the convection in plane AA is due to the smaller pores in the pore tree that are interconnected outside of plane AA. This connectivity will translate into a slower velocity in the pore crossing plane AA but could be significant because 99% of the pores in plane AA are not interconnected in that plane. Fig. 4c illustrates the case where the convection in plane AA is due to the pores in the largest trees that provide a direct link across the porous sample.

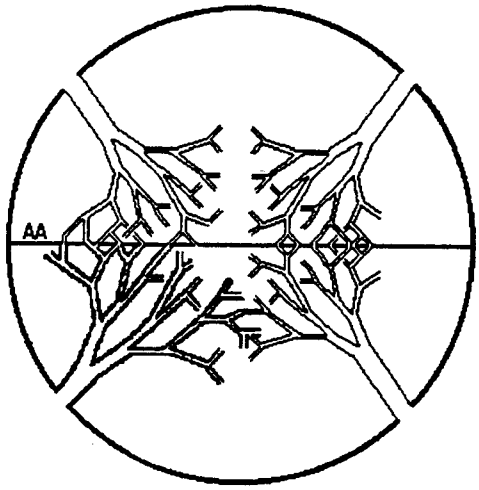

a) Pores Interconnected in Plane AA

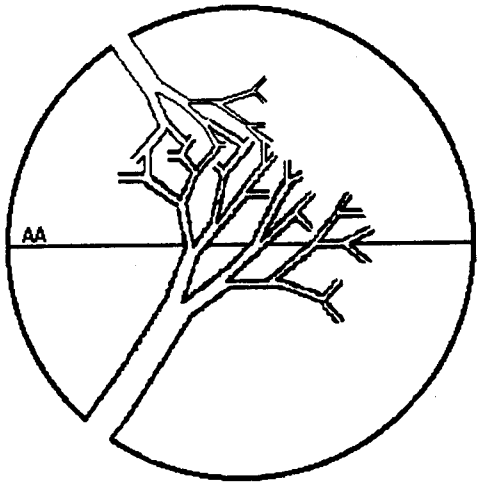

b) Pores Interconnected Out of Plane AA

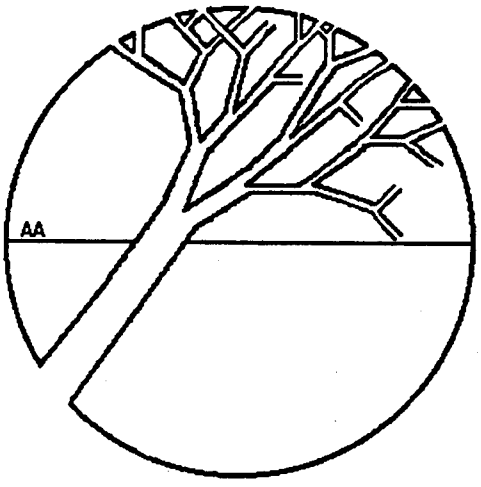

c) Pore Tree Spans the Porous Sample

Fig. 4 Convection in the Pore Tree

The fundamental relationship governing convection in a porous media is Darcy's Law which relates the volume flow rate $\dot{Q}$ to the pore radius r_p and the pressure gradient $\frac{dP}{dx}$

$$\dot{Q} = \frac{\pi r_p^4}{8\mu}\left(-\frac{dP}{dx}\right) \tag{28}$$

where μ is the viscosity of the fluid. Considering an isolated pore tree with n pores at location x within the tree and dr_p/dx as given by Eqs. (15) and (16) respectively, the volume flow rate for the entire tree (n branches) is given by

$$\dot{Q}_{tree} = \frac{\pi r_t^2 r_p^3}{8\mu l_t}\left(\frac{dP}{dr_p}\right) \tag{29}$$

For a constant volume flow rate within the tree, integration of Eq. (28) yields

$$p(r_t) - p(r_p) = \frac{4\dot{Q}_{tree}\mu l_t}{\pi r_t^2}\left(\frac{1}{r_p^2} - \frac{1}{r_t^2}\right) \tag{30}$$

which indicates that extremely large pressures will be required in the tree trunk to maintain the constant volume flow rate in the smaller pores. This suggests that, whenever possible, the flow will "short circuit" through the largest interconnected pores, the pressure gradient will be depicted by the largest pores, and there will be a small but finite flow in the smaller pores.

For the case of $r_t \gg r_p$ and $p(r_t) \gg p(r_p)$, Eq. (30) predicts that the volume flow rate of the tree is limited by the smallest value of r_p to the second power

$$\dot{Q}_{tree} = \frac{\pi r_t^2 p(r_t) r_p^2}{4\mu l_t} \tag{31}$$

while that of a single pore is limited by the value of r_p to the fourth power.

$$\dot{Q}_p = \frac{\dot{Q}_{tree}}{n(x)} = \frac{\pi p(r_t) r_p^4}{4\mu l_t} \tag{32}$$

Comparing Eq. (32) to Eq. (28) suggests that the pressure gradient is depicted solely by the largest pores.

$$\frac{dP}{dx} = \frac{-2\,p(r_t)}{l_t} \tag{33}$$

Hence, flow in the pore tree is consistent with that for a bundle of isolated pores and the volume flow rate within a single pore tree may be used to determine the dominant transport modes identified in Fig. 4.

Consider any pore of radius r_s in plane AA of Fig. 4b to be the trunk of a tree. Each pore of size r_p within the tree possesses the probability $P_I(r_p)$ of being interconnected and each interconnected pore in the tree will carry volume flow rate $\dot{Q}_p(r_p,r_s)$. Since there are $N_s dr_p$ (Eq. 10: $N_s = r_s^3/r_p^4$) pores in size range dr_p within the tree, the total volume flow rate $\dot{Q}_\infty(r_s)$ through trunk r_s in plane AA becomes

$$\dot{Q}_\infty(r_s) = \int_{r_{min}}^{r_s} \dot{Q}_p(r_p,r_s)\; P_I(r_p)\; N_s\, dr_p \tag{34}$$

or, to first order,

$$\dot{Q}_\infty(r_s) = \frac{\theta\pi\, p(r_s)\, r_s^4 \ln(r_{max}/r_s)}{16\,\mu\,\beta\, l_s} + H.O.T \tag{35}$$

Within this approximation, it is seen that $\dot{Q}_\infty(r_s)$ is identical to the volume flowing through the pores that are interconnected within plane AA. i.e.,

$$\dot{Q}_\infty(r_s) \equiv \dot{Q}_p(r_s)\; P_I(r_s) \tag{36}$$

which demonstrates that all volume flow through plane AA in pore size r_s is dominated by the interconnectivity of size r_s in plane AA and not by the interconnectivity of smaller pores in subsequent branches of the pore tree. Simply stated: case 4a dominates case 4b.

Case 4c has not yet been evaluated.

V. SUMMARY

This report is the third technical report on the project entitled "Development of Pore Structure Models for Water and Contaminant Transport in Partially Frozen Soils," submitted to ARO for the period 1 November 1994 to 18 November 1994. The pore tree model is being extended to describe the permeable pore structure which characterizes the subsurface flow of water in soil, the dispersion of contaminants and the in-situ remediation of contaminated sites. Permeability requires a statistical determination the "branches" that are common to several trees to allow percolation through the large scale (mobile) structure in addition to diffusion through the smaller scale (immobile) structure. While permeability is dominated by the largest pores, it is important to determine the level of convection that is occurring at the intermediate scales in order to accurately describe transport. Approximately one percent of all pores are interconnected through larger pores. Hence, convection will be responsible for transport in some of the small pores without influencing the over all permeability. This suggests a very wide range of pore sizes separating the mobile and immobile regions and a complicated mixture of convective and diffusive transport in this pore size range. Subsequent analysis will utilize the interconnectivity of the pores to determine the distribution of the permeability with pore size.

VI. REFERENCES

Ahmed, Usman., Crary, S.F., and Coates, G.R. (1991), "Permeability Estimation: The Various Sources and Their Interrelationships," Proc. Soc. Petroleum Eng., JPT, May 1991, 578-587.

Gavalas, G.R. (1980), "A Random Capillary Model with Application to Char Gasification at Chemically Controlled Rates," AIChE J., 26, 577.

Gavalas, G.R. (1981), "An Analysis of Char Combustion Including the Effect of Pore Enlargement," Comb. Sci. Tech., 24, 197.

Goggin, D.J.; Chandler, M.A.; Kocurek, G.;Lake, L.W.(1992), "Permeability Transects of Eolian Sands and Their Use in Generating Random Permeability Fields", Proc. Soc. Petroleum Eng., Formation Evaluation, March 1992, pp.7-16.

Kothandaraman, G. and Simons, G.A. (1984), "Evolution of the Pore Structure in PSOC 140 Lignite During Pyrolysis," The Combustion Institute, Twentieth Symposium (International) on Combustion, Ann Arbor, MI.

Lewis, P.F. and Simons, G.A. (1979), "Char Gasification: Part II. Oxidation Results," Comb. Sci. Tech., 20, 3 & 4, 117-124.

Simons, G.A. and Finson, M.L. (1979), "The Structure of Coal Char: Part I. Pore Branching," Comb. Sci. Tech., 19, 5 & 6, 217-226.

Simons, G.A. (1979a), "The Structure of Coal Char: Part II. Pore Combination," Comb. Sci. Tech., 19, 5 & 6, 227-235.

Simons, G.A. (1979b), "Char Gasification: Part I. Transport Model," Comb. Sci. Tech., 20, 3 & 4, 107-116.

Simons, G.A. and Rawlins, W.T. (1980), "The Reaction of SO_2 and H_2S with Porous Calcined Limestone," Ind. & Eng. Chem., Process Des. & Dev., 19, 565-572.

Simons, G.A. (1982), "The Pore Tree Structure of Porous Char," The Combustion Institute, Nineteenth Symposium (International) on Combustion, Haifa, Israel.

Simons, G.A. (1983a), "The Role of Pore Structure In Coal Pyrolysis and Gasification," (Invited Survey Article) Progress in Energy and Combustion Science, 9, 269.

Simons, G.A. (1983b), "Coal Pyrolysis I. Pore Evolution Theory," Comb. and Flame, 53, 83-92.

Simons, G.A. (1984), "Coal Pyrolysis II. Species Transport Theory," Comb. and Flame, 55, 181-194.

Simons, G.A., Garman, A.R., and Boni, A.A. (1984), "High Pressure Sulfur Sorption by Limestone," Paper No. 33, Eastern Section of the Combustion Institute, Fall Technical Meeting, Clearwater Beach, FL.

Simons, G.A., Ham, D.O., and Moniz, G.A. (1986), "Catalytic Cracking of Aromatic Hydrocarbons", Physical Sciences Inc. PSI-385/TR-552, DOE/MC/21385-2021.

Simons, G.A. and Garman, A.R. (1986), "Small Pore Closure and the Deactivation of the Limestone Sulfation Reaction," AIChE J., 32, 1491.

Simons, G.A., Garman, A.R., and Boni, A.A. (1987), "The Kinetic Rate of SO_2 Sorption by CaO," AIChE J., 33, 211.

Simons, G.A. (1988), "Parameters Limiting Sulfation by CaO," AIChE J., 34, 167.

Simons, G.A., Parker, T.E., and Morency, J.R. (1988), "The Oxygen Reaction Order of SO_2 with CaO," Comb. & Flame, 74, 107.

Simons, G.A. (1991), "Predictions of CMA Utilization for In-Situ SO_2 Removal in Utility Boilers," International Symposium on Calcium Magnesium Acetate (CMA), Northeastern University, Boston, MA, May 14-16. Also: Resources, Conservation and Recycling, 7, 161-170, 1992.

Simons, G.A., Parker, T.E., Moore, J.W., Senior, C.A., and Levendis, Y.A. (1992), "Combined NO_x/SO_x Control Using a Single Liquid Injection System," Physical Sciences Inc., TR-1169.

Stacy,W.O. and Walker, Jr., P.L. (1972), "Structure and Properties of Various Coal Chars," Coal Research Section, College of Earth and Mineral Sciences, The Pennsylvania State University, PB 233996.